Effect of state-dependent delay on a weakly damped nonlinear oscillator

Jonathan L. Mitchell*
Department of Mathematics, Hardin-Simmons University, Abilene, Texas 79601, USA

Thomas W. Carr†
Department of Mathematics, Southern Methodist University, Dallas, Texas 75275-0156, USA

(Received 12 October 2010; revised manuscript received 19 January 2011; published 15 April 2011)

We consider a weakly damped nonlinear oscillator with state-dependent delay, which has applications in models for lasers, epidemics, and microparasites. More generally, the delay-differential equations considered are a predator-prey system where the delayed term is linear and represents the proliferation of the predator. We determine the critical value of the delay that causes the steady state to become unstable to periodic oscillations via a Hopf bifurcation. Using asymptotic averaging, we determine how the system's behavior is influenced by the functional form of the state-dependent delay. Specifically, we determine whether the branch of periodic solutions will be either sub- or supercritical as well as an accurate estimation of the amplitude. Finally, we choose a few examples of state-dependent delay to test our analytical results by comparing them to numerical continuation.

DOI: 10.1103/PhysRevE.83.046110 PACS number(s): 02.30.Ks, 05.45.−a

I. INTRODUCTION

Delays are used in numerous mathematical models over a wide variety of applications. Examples of constant delays are found in lasers [1,2], machine-tool vibrations [3,4], blood-cell production [5,6], population dynamics [7–9], malarial microparasites [10–13], and many others. In some cases, the effect of a delay is negligible, while in other cases the delay can significantly influence the dynamics, including stability of equilibria and nonlinear effects. Some models incorporate state-dependent delays with the assumption that they describe the physical situation more realistically than their constant-delay predecessors [14–17]. While the methods and theory for constant delay-differential equations (DDEs) are well established [18,19], those for state-dependent delay-differential equations (SDDEs) comprise a growing field of study [20–23]. In this paper we consider a nonlinear oscillator that includes a state-dependent delay. By applying the asymptotic method of averaging, we are able to describe how the functional form of the delay determines the nature of a Hopf bifurcation to persistent oscillations.

The SDDEs we consider are given by Eq. (1), where the constant-delay version has applications in lasers [1,2,24–26], population epidemics [8,9], and malaria infection [10,11]. More generally, we interpret these equations as a predator-prey system with the predator x regulated by a delayed version of the prey population y. The nondimensionalized version of the application-specific model is

$$\begin{aligned} \dot{x} &= y|_\tau - ax, \\ \dot{y} &= -x(1+y), \end{aligned} \tag{1}$$

where $y_\tau = y(t-\tau)$ is the delay, and x and y represent deviations from some nonzero steady state. For example, in disease populations [8,9], the original variables are fractions of susceptible and infectious individuals such that $(x,y) = (0,0)$ represents the nontrivial endemic state. The parameter a represents the weak dissipation of the system such that $a \ll 1$ and the trajectories spiral toward the origin as $t \to \infty$. In this way for $\tau = 0$ Eq. (1) form a weakly damped nonlinear oscillator. More specifically, for $a = 0$ and $\tau = 0$ the undamped system of ordinary differential equations (ODEs) is conservative with energy given by

$$E(x,y) = \tfrac{1}{2}x^2 + y - \ln|1+y|. \tag{2}$$

In Fig. 1 we show periodic orbits in the phase plane where each orbit corresponds to a different energy. We note that one cycle of trajectory (a) consists of a sharp pulse for y followed by a longer latency period when y is near but slightly greater than -1; in the original physical variables (not presented) this corresponds to the prey population being near zero. During the pulsation for y, the predator population x increases quickly, followed by a slow decay during the latent period. As stated above, when $a > 0$ the oscillations are damped and the system spirals to the steady state. For sufficiently large τ, oscillations become excited and self-sustained via a Hopf bifurcation.

We are interested in the case where the delay is dependent on one the state variables, which can occur in a number of different ways. In the case of machine-tool vibrations, nonconstant delays can be the result of uneven drilling [14,27,28]. These models typically exhibit implicitly defined delays, and their study relies on numerical computation. However, explicitly defined delays can also be incorporated into mathematical models. In a model for the economics of fishing, the delay representing a fisherman's reaction time to fluctuations in economic rent can exhibit linear and even nonlinear dependencies on harvesting efforts and population size [7]. As another example, in Ref. [15] a biological model for erythropoiesis incorporates a nonmonotonic state-dependent (SD) delay as a state variable representing the lifespan of mature erythrocytes.

In this paper, we consider the delay in Eq. (1) to be a function of y such that $\tau = \tau(y)$ for the following hypothetical arguments. In Ref. [10], y represents parasite load for a malarial infection and causes the host's immune effectors, represented by x, to respond to the parasite. In this context,

*Jonathan.L.Mitchell@hsutx.edu
†tcarr@smu.edu

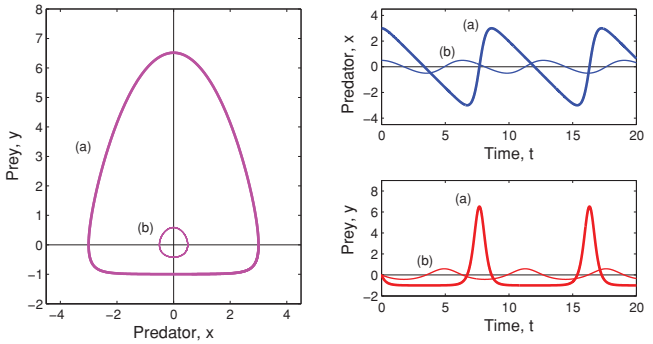

FIG. 1. (Color online) The phase plane (left) and time series (right) for the undamped ($a = 0$) and instantaneous ($\tau = 0$) system given by Eq. (1) are numerically computed with initial conditions (a) $y(0) = 0$ and $x(0) = 3$ (thick curve) and (b) $y(0) = 0$ and $x(0) = 1/2$ (thin curve). Large-amplitude oscillations (a) exhibit a pulsating solution and correspond to high energy defined by Eq. (2), while small-amplitude oscillations (b) are sinusoidal.

the delay in Eq. (1) represents a time lag in production of immune effectors, which we consider to be influenced by the parasite load. Alternatively, in an SI-epidemic model [8,9] y is the infectious class, x is the susceptible class, and there is an infectious-load dependent delay in the contact process that removes individuals from the susceptible class. Concerning the functional form of $\tau(y)$, we consider certain restrictions to be appropriate for applications of the model, namely, that it remain a smooth positive function in a neighborhood near the steady-state value $y = 0$. We do not, however, restrict the slope or shape of $\tau(y)$, which might limit its application.

In the next section, we begin by analyzing the linear stability of the zero steady state and find the size of delay necessary to cause an instability via a Hopf bifurcation. For small damping, the delay required to produce a limit cycle is also small. We use averaging to determine how the amplitude and frequency of the limit-cycle solutions depend on the size and functional form of the state-dependent delay. We find that the branch of delay-induced periodic solutions can be either supercritical or subcritical depending on the functional form of the delay. Finally, we consider different examples of $\tau(y)$ and examine properties that influence the branch of periodic solutions and compare our results to those generated from numerical continuation [29]. We conclude with a discussion of the paper's results.

II. LINEAR STABILITY

In this section we examine the stability of the zero steady state by linearizing Eq. (1) and deriving the characteristic equation for the growth rates. A fundamental problem in the stability analysis of SDDEs is how to properly treat the state-dependent delay. In particular, differentiability of the dependent variable is an issue, so any expansions involving derivatives become questionable. Nevertheless, we will use the heuristic approach of evaluating the delay at the desired steady state to obtain a constant delay and then linearize. For the case where the delay is an explicit function of the state and, roughly speaking, the function is continuously differentiable, this approach has been shown to generate the correct approximating system [21]. In the next section we use a Taylor-series approximation for the delay evaluated near the steady state and, thus, require $\tau(y)$ to be formally smooth. Because $y = 0$ is the steady state under consideration, the delay takes the constant value $\tau(0) = \tau_0$, which yields $y|_\tau \approx y|_{\tau_0}$. Then the linear system is

$$\begin{aligned} \dot{x} &= y|_{\tau_0} - ax, \\ \dot{y} &= -x, \end{aligned} \tag{3}$$

which has a characteristic equation given by

$$F(\lambda,\tau) = \lambda^2 + a\lambda + e^{-\lambda\tau_0} = 0. \tag{4}$$

In the case that $\tau = 0$ and for $a \ll 1$, the zero steady state is a stable focus with complex-conjugate eigenvalues given by

$$\lambda = -\frac{a}{2} \pm \sqrt{\left(\frac{a}{2}\right)^2 - 1} \sim -\frac{a}{2} \pm i\left(1 - \frac{a^2}{8}\right). \tag{5}$$

We now consider nonzero delay $\tau(0) = \tau_0 \neq 0$ and note that Eq. (4) contains the exponential term $\exp(-\lambda\tau_0)$. We look for a Hopf bifurcation by substituting $\lambda = i\omega$ into Eq. (4) and obtain

$$\begin{aligned} 0 &= -\omega^2 + \cos(\omega\tau_0), \\ 0 &= a\omega - \sin(\omega\tau_0). \end{aligned} \tag{6}$$

After some algebra we find that the steady state bifurcates to a branch of delay-induced periodic solutions with frequency and delay satisfying

$$\begin{aligned} \omega = \omega_h &\equiv \sqrt{-\frac{a^2}{2} + \sqrt{\left(\frac{a^2}{2}\right)^2 + 1}} \sim 1 - \frac{a^2}{4}, \\ \tau_0 = \tau_h &\equiv \frac{1}{\omega_h}\arctan\left(\frac{a}{\omega_h}\right) \sim a. \end{aligned} \tag{7}$$

We note that the middle portions of Eq. (7) are exact expressions while the right-hand sides are asymptotic approximations when $a \ll 1$. The latter indicates that the delay required to excite persistent oscillations is of the same order of magnitude as the weak damping and that the frequency of the oscillations is less than when the delay is zero, as shown in Eq. (5).

III. BIFURCATION EQUATION

In this section we use averaging, in the formal sense, to derive a bifurcation equation that indicates how the amplitude of periodic oscillations that appear at the Hopf bifurcation depend upon the parameters. Averaging [30,31] requires that the system flow has some degree of differentiability, and this is not *a priori* guaranteed for SDDEs [21]. Nevertheless, we forge ahead with our heuristic approach and, in the end, find that we have excellent fit between the results of our analysis and those generated from numerical simulations. Our approach follows closely that which has been done for ODE and DDE versions of Eq. (1), which uses the system's energy as the new dependent variable of interest [24,32].

We begin by imposing small damping such that $a = \epsilon\tilde{a}$ with $\epsilon \ll 1$. From the linear-stability analysis in Sec. II, we have determined that the critical delay time at the Hopf bifurcation is

$O(\epsilon)$. Thus, we let $\tau(y) = \epsilon\tilde{\tau}(y)$ so that $y[t - \tau(y)] = y[t - \epsilon\tilde{\tau}(y)]$. For $\epsilon = 0$ we have the conservative, nonlinear ODEs:

$$\begin{aligned} \dot{x_0} &= y_0, \\ \dot{y_0} &= -x_0(1 + y_0), \end{aligned} \tag{8}$$

which we will refer to as the *unperturbed system*. The conserved energy of the unperturbed system is given by Eq. (2), which we reproduce here:

$$E(x, y) = \tfrac{1}{2}x_0^2 + y_0 - \ln|1 + y_0|. \tag{9}$$

For $\epsilon = 0$ it is a simple matter to check that $dE/dt = 0$. For $\epsilon \neq 0$ the damping and the delay cause the energy to evolve in time. The basic idea of averaging is to evaluate the result for dE/dt, $\epsilon \neq 0$, using the unperturbed system with $x = x_0$ and $y = y_0$ from Eq. (8), and to integrate (average) over one period (P) of oscillation. The result is

$$\frac{dE}{dt} = \frac{1}{P}\int_0^P \{[y_0(t - \epsilon\tilde{\tau}) - y_0(t)] - \epsilon\tilde{a}x_0(t)^2\}\, dt, \tag{10}$$

where we have implicitly assumed that $|y_0(t - \epsilon\tilde{\tau}) - y_0(t)| = O(\epsilon)$. Periodic solutions exist if, after one period, the change in energy is zero ($dE/dt = 0$) so that we have the bifurcation equation

$$0 = \frac{1}{P}\int_0^P ([y_0\{t - \epsilon\tilde{\tau}(y_0)] - y_0(t)\} - \epsilon\tilde{a}x_0(t)^2)\, dt. \tag{11}$$

Before we continue, we formally evaluate the delay term. Specifically, we let

$$y_0[t - \epsilon\tilde{\tau}(y_0)] = y_0(t) - \epsilon\tilde{\tau}(y_0)\dot{y_0}(t) + O(\epsilon^2). \tag{12}$$

After substituting for $\dot{y_0}$ from Eq. (8) and keeping only the $O(\epsilon)$ terms, we have

$$0 = \frac{1}{P}\int_0^P \left[\tau(y_0)x_0^2(1 + y_0) - ax_0^2\right] dt, \tag{13}$$

where we have reabsorbed the ϵ into the definitions for τ and a.

The challenge at this point is to evaluate the integral. Because explicit solutions to Eq. (8) cannot be obtained, we use Linstedt's method [32] to find small-amplitude approximations given by

$$\begin{aligned} x_0 &= R\cos\omega t - \frac{1}{6}R^2\sin 2\omega t - \frac{1}{32}R^3\cos 3\omega t + O(R^4), \\ y_0 &= -\omega R\sin\omega t - \frac{1}{3}R^2\cos 2\omega t + \frac{3}{32}R^3\sin 3\omega t + O(R^4), \\ \omega &= 1 - \frac{R^2}{24} + O(R^4), \end{aligned} \tag{14}$$

where $R \sim x_{\max}$. Under the assumption that y_0 is of small amplitude, we then expand the state-dependent delay term as

$$\tau(y_0) = \tau_0 + \tau_y y_0 + \frac{1}{2}\tau_{yy}y_0^2 + O\left(y_0^3\right). \tag{15}$$

The expressions τ_0, τ_y, and τ_{yy} represent the delay, its derivative, and second derivative, respectively, where each is evaluated at the steady-state solution, $y = 0$. We find that keeping the $O(y_0^2)$ terms is sufficient to obtain good fit with numerical simulations. We then substitute Eqs. (14) and (15) into Eq. (13), integrate over one period $[0,2\pi]$, and the result is

$$0 = \tfrac{1}{2}(\tau_0 - a) + \tfrac{1}{8}R^2\left(\tau_y + \tfrac{1}{2}\tau_{yy}\right) + O(R^4). \tag{16}$$

Finally, we solve for R to obtain

$$R = 2\sqrt{-\frac{\tau_0 - a}{\tau_y + \frac{1}{2}\tau_{yy}}}. \tag{17}$$

We note that a is the leading-order approximation to the value of the delay at the Hopf bifurcation [see Eq. (7)] and that R is the amplitude of x. Thus, we write that

$$x_{\max} = 2\sqrt{-\frac{\tau_0 - \tau_h}{\psi}}, \tag{18}$$

where

$$\psi = \tau_y + \tfrac{1}{2}\tau_{yy}. \tag{19}$$

The expression under the radical in Eq. (18) must be nonnegative. Thus, if $\tau_0 - \tau_h > 0$ (<0), then we require $\psi < 0$ (>0). From the linear stability analysis we know that when $\tau_0 - \tau_h > 0$ the steady state is unstable. This suggests that if $\psi < 0$ such that the branch of periodic solutions continues for $\tau_0 - \tau_h > 0$, then those periodic solutions will be stable corresponding to a supercritical bifurcation. Similarly, if $\psi > 0$, the branch of periodic solutions that continue for $\tau_0 - \tau_h < 0$ is expected to be unstable corresponding to a subcritical bifurcation. In the next section, we will choose a few examples of state-dependent delay and demonstrate the validity of Eqs. (18) and (19), as well as confirm that the stability of the periodic solutions is consistent with the above discussion.

We note that ψ depends only on the first and second derivatives for $\tau(y)$ because the higher-order derivatives have been neglected in Eq. (15) under the assumption that for small-amplitude oscillations they are small. It should also be noted that when $\psi = 0$ Eq. (18) is singular and corresponds to losing the amplitude-dependent term in Eq. (16). This requires that the perturbation analysis be continued to higher order to obtain the $O(R^4)$ term. We discuss this further in the next section when we consider the case of constant delay.

IV. EXAMPLES

In this section, we consider various definitions of the state-dependent delay and examine how the properties of each influence the branch of periodic solutions stemming from the Hopf bifurcation. In addition, we demonstrate how the bifurcation results of the previous section accurately predict nonlinear behavior for Eq. (1) with state-dependent delay. In each case, we use $\tau_0 > 0$ as the bifurcation parameter because it measures the *strength* of the delay. In other words, we define the state-dependent delay such that τ_0 is the delay where y is at its steady state ($y = 0$). The parameter ρ will be used as a free parameter to change the slope or shape of each example function. We note that the linear stability of the trivial steady state is identical for each definition of $\tau(y)$ in this section. In

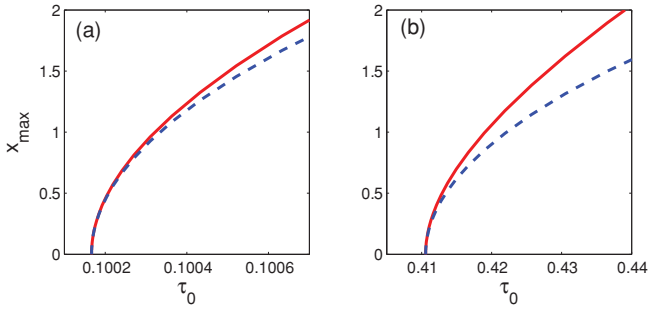

FIG. 2. (Color online) The constant delay yields a supercritical branch of periodic solutions with damping given by (a) $a = 0.1$ and (b) $a = 0.4$. Numerical continuation (solid) is compared to our results given by Eq. (20) (dashed). We note that the scaling for τ_0 in (a) is much smaller than that for τ_0 in Figs. 3–5, indicating that the curve here is relatively steep or nearly vertical.

other words, the Hopf bifurcation occurs at the same delay given by Eq. (7).

A. Constant delay

We begin by considering a constant time lag $\tau(y) = \tau_0$ as a reference to compare against when we discuss examples with state-dependent delay. Because $\tau_y = \tau_{yy} = 0$, we note that ψ is zero such that Eq. (18) is singular. In general, this indicates that the perturbation method must be carried out to higher order in the small parameter. Unfortunately, higher-order averaging would be very difficult for the present problem. However, we have previously analyzed the constant delay case for a very similar model as Eq. (1) in Ref. [10]. More specifically, we look for small-amplitude solutions from the outset and look for solutions of the form $x = \eta x_1 + \eta^2 x_2 + \cdots$, $\eta \ll 1$, focus near the Hopf bifurcation with $\tau = \tau_h + \eta^2 \tau_2$, and introduce an additional slow time $\eta^2 t$. By continuing the perturbation method to $O(\eta^2)$ we obtain a solvability condition, which we analyze to obtain

$$x_{\max} \sim 2\sqrt{\frac{3(\tau_0 - \tau_h)}{2a^3}}, \tag{20}$$

indicating that the branch of periodic solutions is supercritical. The denominator of Eq. (20) is proportional to a^3 such that for small damping the amplitude is very large. In general, we will see that the bifurcation curve for the constant-delay case is steeper than for state-dependent delay. As shown in Fig. 2, Eq. (20) exhibits good fit with numerical continuation [29] for small-amplitude solutions. We note that our approximation in Eq. (20) improves when the damping is decreased because we derived it for $a \ll 1$. This explains why the dashed line in Fig. 2(a) ($a = 0.1$) is closer to the numerical result than that in Fig. 2(b) ($a = 0.4$).

B. Sigmoid

The first state-dependent delay we consider, which we refer to as the *sigmoid* case, is defined by

$$\tau(y) = 2\tau_0 \frac{1}{1 + e^{\rho y}}. \tag{21}$$

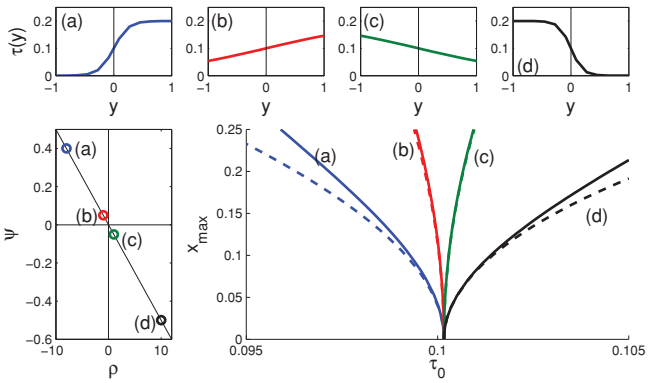

FIG. 3. (Color online) (top) The sigmoid state-dependent delay $\tau(y)$ given by Eq. (21) is plotted as a function of y for (a) $\rho = -8$, (b) $\rho = -1$, (c) $\rho = 1$, and (d) $\rho = 10$. (bottom-left) ψ is given by Eq. (22) for $\rho \in [-10, 12]$ and indicated points corresponding to delay definitions (a)–(d). (bottom-right) Numerical continuation [29] (solid curves) along with our bifurcation equation given by Eq. (18) (dotted curves) illustrate sub- and supercritical branches of periodic solutions corresponding to (a) and (b) where $\psi > 0$ versus (c) and (d) where $\psi < 0$.

This definition of $\tau(y)$ has range $(0, 2\tau_0)$ and domain $(-\infty, \infty)$ such that the delay is defined and positive regardless of the value of the state variable y. The parameter ρ can be any nonzero number because $\rho = 0$ corresponds to the constant-delay case. It follows from Eq. (21) that for the sigmoid case

$$\psi = \tau_y = -\frac{\tau_0 \rho}{2}, \tag{22}$$

which is positive when $\rho < 0$, indicating that the Hopf bifurcation is subcritical, as shown in Figs. 3(a) and 3(b). On the other hand, $\psi < 0$ when $\rho > 0$, causing the bifurcation to be supercritical, as shown in Figs. 3(c) and 3(d). As $\rho \to 0$, $\tau(y)$ approaches the constant function, which causes $\psi \to 0$ as indicated by Figs. 3(b) and 3(c). As a consequence, the amplitude of periodic solutions, which is inversely proportional to $\sqrt{|\psi|}$, increases for delays near the Hopf bifurcation.

C. Parabolic

In this section, we consider a *parabolic* state-dependent delay defined by

$$\tau(y) = \tau_0(1 - \rho y^2), \tag{23}$$

which is quadratic in y. As in the previous example, we exclude $\rho = 0$, which yields the constant delay (Sec. IV A). It is clear that when $\rho > 0$, $\tau(y)$ is concave down with domain $[-1/\sqrt{\rho}, 1/\sqrt{\rho}]$. We require that $\rho < 1$ in order to maintain positive delay for small-amplitude solutions. On the other hand, when $\rho < 0$, $\tau(y)$ is concave up and, thus, always positive. It follows from Eqs. (23) and (19) that

$$\psi = \tfrac{1}{2}\tau_{yy} = -\tau_0 \rho, \tag{24}$$

which is linear in ρ with negative slope. Thus, we find that the Hopf bifurcation is subcritical where $\rho < 0$ as shown in Figs. 4(a) and 4(b), while it is supercritical when $\rho > 0$ as illustrated in Figs. 4(c) and 4(d).

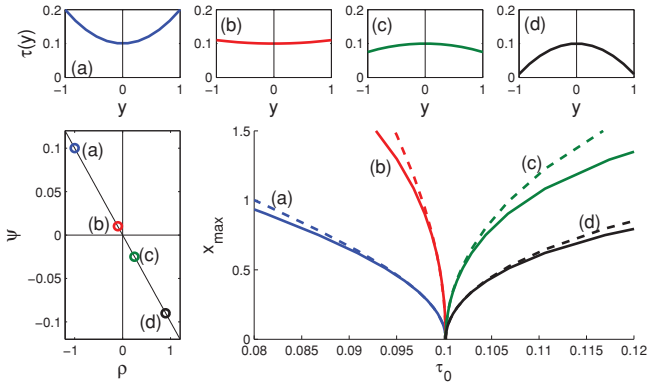

FIG. 4. (Color online) (top) The parabolic state-dependent delay $\tau(y)$ is given by Eq. (23) and (a) $\rho = -1$, (b) $\rho = -0.1$, (c) $\rho = 0.25$, and (d) $\rho = 0.9$. (bottom-left) ψ is given by Eq. (24) for $\rho \in [-1.2, 1.2]$ and indicated points corresponding to delay definitions (a)–(d). (bottom-right) Like Fig. 3, numerical continuation [29] (solid curves) is plotted with our analytical result given by Eq. (18) (dotted curves) for (a) and (b) where $\psi > 0$ versus (c) and (d) where $\psi < 0$.

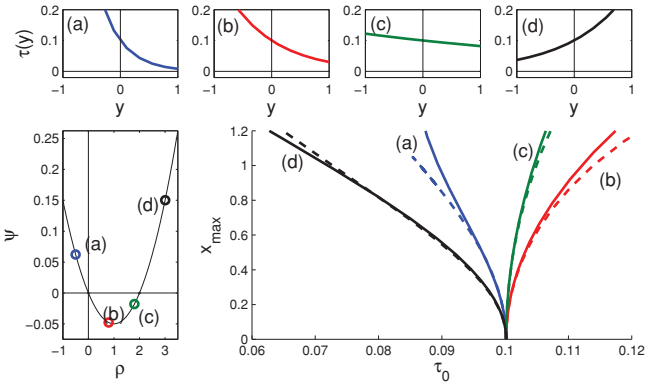

FIG. 5. (Color online) (top) The exponential state-dependent delay $\tau(y)$ is given by Eq. (26) and (a) $\rho = -0.5$, (b) $\rho = 0.8$, (c) $\rho = 1.8$, and (d) $\rho = 3$. (bottom-left) ψ is given by Eq. (27) for $\rho \in [-1, 3.5]$ and indicated points corresponding to delay definitions (a)–(d). (bottom-right) Numerical continuation [29] (solid curves) is plotted with our analytical result given by Eq. (18) (dotted curves) for (a) and (d) where $\psi > 0$ versus (b) and (c) where $\psi < 0$.

While for the sigmoid case ψ depends on τ_y by Eq. (22), for the parabolic case ψ depends on τ_{yy} by Eq. (24), indicating the importance of the latter term in the definition of ψ in Eq. (19). For both the parabolic and sigmoid cases, we note that their respective definitions of ψ are linear in ρ as shown in Figs. 3 and 4. The next example will show a case where $\psi \sim \rho^2$.

D. Exponential

In both previous examples, the change from subcritical to supercritical occurs when the delay is a constant and $\psi = 0$. Here we look for nonconstant delays yielding $\psi = 0$. Although the expressions τ_y and τ_{yy} are evaluated at $y = 0$, we use $\psi = 0$ as motivation to form the initial value problem (IVP):

$$\tau'(y) + \tfrac{1}{2}\tau''(y) = 0, \quad \tau(0) = \tau_0, \quad \tau'(0) = k. \tag{25}$$

The solution to this IVP is $\tau(y) = \tau_0 + \frac{1}{2}k - \frac{1}{2}k\exp(-2y)$. We choose $k = -2\tau_0$ for convenience to obtain the simpler expression $\tau(y) = \tau_0 \exp(-2y)$. We now introduce the parameter ρ in order to tune the delay so that the right-hand side of Eq. (25) could be positive or negative instead of strictly zero. More specifically, we consider delay defined by

$$\tau(y) = \tau_0 e^{(\rho-2)y} \tag{26}$$

and refer to it as the *exponential* case. $\tau(y)$ is decreasing when $\rho < 2$ and increasing when $\rho > 2$, while $\rho = 2$ corresponds to a constant delay. In this case, both τ_y and τ_{yy} are nontrivial such that

$$\psi = \tau_0\rho\left(\tfrac{1}{2}\rho - 1\right). \tag{27}$$

Unlike the sigmoid and parabolic delays, the exponential delay causes ψ to be quadratic in ρ with zeros at $\rho = 0$ and 2, and vertex $(1, -\tau_0/2)$. It follows that the Hopf bifurcation will be subcritical when $\rho < 0$ or $\rho > 2$ because these are the regions where $\psi > 0$, as illustrated by Figs. 5(a) and 5(d). Contrarily, it will be supercritical when $0 < \rho < 2$, as shown in Figs. 5(b) and 5(c).

We note that the zeros of ψ given by $\rho = 0$ and 2 correspond to qualitatively different state-dependent delays. Because $\tau(y)$ is constant when $\rho = 2$, it follows that the bifurcation curve will be supercritical and approximated by Eq. (20). On the other hand, when $\rho = 0$, ψ is zero for nontrivial τ_y and τ_{yy}, yet the delay is a decaying exponential, as illustrated in Figs. 5(a) and 5(b). In this case, the nonlinear effect of the delay is captured at higher order.

Consider the four cases of (ρ, ψ) as shown Fig. 5, each of which corresponds to a different $\tau(y)$ shown at the top. In Fig. 5(a), we see for $\rho < 0$ that $\tau(y)$ is a decreasing function and ψ is positive, yielding a subcritical bifurcation. If we adjust ρ to be positive, as shown in Fig. 5(b), then ψ is negative, indicating the bifurcation has switched to supercritical. As we approach $\rho = 2$ as shown in Fig. 5(c), ψ remains negative (bifurcation remains supercritical), but the amplitude of oscillations is greater. This is because $|\psi|$ at (b) is greater than that at (c), causing the coefficient for amplitude in Eq. (18) to be larger for (c). Furthermore, the amplitude of persistent oscillations for the supercritical case will be minimized when ψ is at its local minimum, i.e., $\rho = 1$ and $\psi = -\tau_0/2$. For values of $\rho > 2$, ψ is positive once again, causing the bifurcation to be subcritical, as shown in Fig. 5(d). Finally, we note that the amplitude of periodic solutions for the two subcritical cases in Fig. 5 is larger where ψ is smaller.

V. DISCUSSION

Our analysis applies the asymptotic method of averaging to a delay-differential equation with state-dependent delay. We employ a series expansion of the functional delay based on small-delay and small-amplitude oscillations. While our approach is formal and there is no *a priori* guarantee this method will produce correct results, we find that the derived bifurcation equation correctly describes what is observed using numerical continuation [29]. Further, we have also simulated the SDDEs directly [33] and obtained identical results.

The results of our analysis allow us to predict how the functional form of the state-dependent delay, $\tau(y)$, influences the nonlinear behavior of the system. Specifically, the sign of the quantity $\psi = \tau_y(0) + (1/2)\tau_{yy}(0)$ determines whether the bifurcation will be supercritical or subcritical. Additionally, ψ controls the amplitude of the periodic solutions such that the amplitude is proportional to $1/\sqrt{|\psi|}$; thus, smaller $|\psi|$ leads to larger amplitude oscillations. The importance of this prediction lies in the different way oscillatory solutions will appear as the delay is increased beyond the value at the Hopf bifurcation point. For the supercritical case, the oscillations will initially be small amplitude and grow smoothly with the distance away from the bifurcation point. In contrast, for the subcritical case increasing the delay past the critical value causes the oscillations to suddenly jump to an attractive limit set consisting of large-amplitude pulsating, quasiperiodic, or chaotic oscillations. In the case of machine-tool vibrations when there is a subcritical bifurcation, increasing the bifurcation parameter past the Hopf bifurcation point leads to chaotic oscillations, referred to as "chatter," which can cause poor surface quality on the material being cut [3] or failure of the cutting tool [28].

In the context of machine-tool vibrations sub- and supercritical Hopf bifurcations have been shown to occur by varying the functional form of the state-dependent delay [14,27]. Although the state-dependent delay in Ref. [14] is implicitly defined, Insperger *et al*. demonstrate that increasing the feed rate, which is proportional to the mean time delay, causes the Hopf bifurcation to switch from sub- to supercritical. In Ref. [27] Demir *et al*. use a Lyapunov-Schmidt reduction to derive a bifurcation equation that depends on the parameters and functional form of their model and obtain a simple condition for either a supercritical or subcritical Hopf bifurcation. However, their result depends in a complex way on the mean delay so that results are not as easy to summarize as our simpler model, which depends on the quantity ψ.

Using the examples in Sec. IV, we demonstrated specific cases of how ψ controls the direction of the bifurcation and, more specifically, that $\psi = 0$ is the critical value that separates supercritical from subcritical bifurcations. There are two different ways in which $\psi = 0$. The delay can be a constant such that $\tau(y) = \tau_0$ and all derivatives are 0, or the functional form can be such that the first and second derivatives balance leading to $\psi = 0$. In Figs. 3 and 4 we show the case when ψ passes through zero with a constant delay. In Fig. 3(b) $\tau(y)$ has positive slope while in Fig. 3(c) it has negative slope, which causes the bifurcation to switch from subcritical to supercritical. In Fig. 4(b), the concavity is positive while in Fig. 4(c) it is negative, which again causes the bifurcation to switch from sub- to supercritical. In contrast, we show in Fig. 5 a change in bifurcation for the case of a nonconstant delay. Specifically, the delay is an exponential function whose derivatives are such that ψ passes through 0. Thus, in both Figs. 5(a) and 5(b) the function is decreasing and concave up, i.e., they are qualitatively similar; however, the size of the derivatives has changed, causing a switch from sub- to supercritical.

We note that the exponential case shown in Fig. 5 is not the only function with nonzero derivatives causing a switch in the direction of the bifurcation. We used the exponential function because it solves the initial-value problem in Eq. (25). However, other examples such as $\tau(y) = \tau_0/(1 + \rho y)$ yield quadratic expressions for ψ as a function of ρ and will exhibit qualitatively similar bifurcation behavior.

For the exponential case in Sec. IV D, we find a number of examples where the subcritical bifurcation branch reaches a turning point and then bends back to the right. The turning point coincides with a change in stability, and in the examples we consider we have verified with numerical continuation [29] and direct solvers [33] that the periodic oscillations beyond the turning point are stable. This then leads to a region of bistability between the turning point on the left and the Hopf bifurcation point on the right, where both the zero steady state and the periodic solutions are stable.

In conclusion, we have successfully applied the asymptotic method of averaging to a relatively simple delay-differential equation with state-dependent delay. Models with state-dependent delays are of increasing interest both because they arise naturally and because they are introduced as part of a broader control methodology. We are able to correctly predict bifurcations to oscillatory solutions in a model that has wide application. Our analytical results are tested against both numerical continuation and direct simulation, and we obtain excellent agreement.

[1] D. Pieroux and T. Erneux, Phys. Rev. A **53**, 2765 (1996).
[2] T. W. Carr, I. B. Schwartz, M. Y. Kim, and R. Roy, SIAM J. Dyn. Syst. **5**, 699 (2006).
[3] T. Kalmar-Nagy, G. Stepan, and F. C. Moon, Nonlinear Dynam. **26**, 121 (2001).
[4] T. Kalmar-Nagy and F. C. Moon, in *Mode-Coupled Regenerative Machine Tool Vibrations* (Wiley-VCH, New York, 2004), pp. 129–149.
[5] M. C. Mackey and J. Milton, Comment Mod. Biol.: Comment Theoret. Biol. **1**, 299 (1990).
[6] L. Pujo-Menjouet and M. C. Mackey, C. R. Biol. **327**, 235 (2004).
[7] Jacques Belair, Lect. Notes Biomath. **92**, 16 (1991).
[8] I. B. Schwartz and H. L. Smith, J. Math. Biol. **18**, 233 (1983).
[9] M. L. Taylor and T. W. Carr, J. Math. Biol. **59**, 841 (2009).
[10] J. L. Mitchell and T. W. Carr, Bull. Math. Biol. **72**, 590 (2010).
[11] J. L. Mitchell and T. W. Carr, J. Biol. Dynam. (2010).
[12] D. Gurarie, P. A. Zimmerman, and C. H. King, J. Theor. Biol. **240**, 185 (2006).
[13] F. E. McKenzie and W. H. Bossert, J. Theor. Biol. **188**, 127 (1997).
[14] T. Insperger, D. A. W. Barton, and G. Stepan, Int. J. Nonlin. Mech. **43**, 140 (2008).
[15] J. M. Mahaffy, J. Belair, and M. C. Mackey, J. Theor. Biol. **190**, 135 (1998).
[16] Jacques Belair, Can. Appl. Math. Q. **6**, 305 (1998).

[17] Jacques Belair, Lect. Notes Pure Appl. Math. **131**, 165 (1991).
[18] J. Hale, *Theory of Functional Differential Equations* (Springer-Verlag, New York Inc., 1977).
[19] N. MacDonald, *Biological Delay Systems: Linear Stability Theory* (Cambridge University Press, Cambridge, UK, 1989).
[20] F. Hartung, J. Comput. Appl. Math. **174**, 201 (2005).
[21] F. Hartung, T. Krisztin, H-O. Walther, and J. Wu, in *Handbook of Differential Equations: Ordinary Differential Equations*, edited by F. Battelli and M. Feckam, Vol. III (Elsevier), p. 435.
[22] H. Walther, J. Diff. Eq. **244**, 1910 (2008).
[23] L. Wang, J. Comput. Appl. Math. **228**, 226 (2009).
[24] T. W. Carr, L. Billings, I. B. Schwartz, and I. Triandaf, Physica D **147**, 59 (2000).
[25] D. Pieroux, T. Erneux, and K. Otsuka, Phys. Rev. A **50**, 1822 (1994).
[26] T. Erneux and P. Mandel, Phys. Rev. A **52**, 4137 (1995).
[27] A. Demir, A. Hasanov, and N. S. Namachchivaya, Int. J. Nonlin. Mech. **41**, 464 (2006).
[28] C. Germay, V. Denoel, and E. Detournay, J. Sound Vib. **325**, 362 (2009).
[29] K. Engelborghs, T. Luzyanina, and G. Samaey, *DDE-BIFTOOL v. 2.00 User Manual: A MATLAB Package for Bifurcation Analysis of Delay Differential Equations* (2001).
[30] J. A. Sanders and F. Verhulst, *Averaging Methods in Nonlinear Dynamical Systems*, Vol. 59 of Applied Mathematical Sciences (Springer-Verlag, New York, 1985).
[31] J. Kevorkian and J. D. Cole, *Multiple Scale and Singular Perturbation Methods* (Springer-Verlag, New York, 1996).
[32] T. Erneux, S. M. Baer, and P. Mandel, Phys. Rev. A **35**, 1165 (1987).
[33] S. Thompson and L. F. Shampine, Appl. Numer. Math. **56**, 503 (2006).